Beryllium reduction potential in AlMg cast alloys

[1]J. Steglich, [1]A. Basa, [2]A. Kvithyld, [2]N. Smith [1]I. Zerbin
[1]TRIMET Aluminium SE, Aluminiumallee 1, 45356 Essen, Germany
[2]SINTEF Industry, Alfred Getz Vei 2, 7034 Trondheim, Norway

Keywords: Beryllium, aluminium-magnesium, cast alloys, health safety and environment

Abstract

Beryllium is used in many aluminium-magnesium alloys to minimize molten metal oxidation and oxide entrainment. As beryllium containing dust and fumes have detrimental effects on health, its use has to be limited. The reduction potential of beryllium has been investigated for AlMg3, AlMg5 and AlMg10 cast alloys as well as Al99,85 as reference material by thermogravimetric analysis (TGA). The samples were alloyed with Be contents between 2 – 57 ppm to measure the oxidation inhibiting effect over time. During TGA, the weight gain by oxidation of each sample was measured continuously for 21 hours at 750 °C in laboratory scale. The results show that the Be inhibiting effect is lost after a period of time. The samples were analysed by X-ray Photoelectron Spectroscopy (XPS), Auger Electron Spectroscopy (AES) and electron microscopy (SEM) to further understand the oxidation mechanism. Finally, the results were used to derive a predictive model for the required Be content to protect an AlMg alloy.

Background

Aluminium-magnesium (AlMg) cast alloys are highly corrosion resistant, suitable for anodising and are therefore often used for visible parts as fittings and naval structures. [1] During alloy production and casting, AlMg melts must be protected against oxidation. Oxide entrainment has to be avoided, as the surface quality, mechanical properties and melt fluidity are depending on metal cleanliness [1,2]. Alloying beryllium to AlMg melts significantly reduces their oxidation and dross formation behaviour. A beryllium content of 0.001 – 0.005 wt% is reported to slow the oxidation rate [3,4], but a description of the effect over time is missing.

Despite its positive effect on oxidation, the use of beryllium has to be limited, as beryllium-containing dust and fumes are toxic as well as cancerous by exposure to the skin and respiratory system. [5] The beryllium content of AlMg alloys is limited in European norm EN 1706 to 0.005 wt% for alloys containing more than 3 wt% magnesium. [6] In the US, the chemical composition limits and designations of castings and ingots are recorded in the so-called “Pink Sheets”. For most of the AA5xx.x AlMg cast alloys, beryllium is not specified and falls under Others Each with up to 0.05 wt%. Only two of these alloys have composition limits between 0.003 – 0.007 wt% Be. [7] The present study suggests that the Be values could be updated to lower composition limits. Although research is continuing [8], no alternative alloying element with comparable performance has been found yet. It is the aim of this work to reduce the beryllium concentration in AlMg cast alloys to a minimum, based on empiric data.

Previous work

The oxidation rate of AlMg alloys with 3 – 20 wt% magnesium and 5 – 200 ppm beryllium was investigated extensively by [9]. The experiments were performed with a similar sample size of 27 ± 0.1 g and an initial surface area of 8.5 cm². Each sample was heated in a vertical tube induction furnace, in argon or air atmosphere to 700 °C or 800 °C. The samples had to be heated up to 170 hours (1 week) to reach a steady state after complete magnesium oxidation, depending on the beryllium content. It was found that all alloys formed Al_2MgO_4 spinel and not only MgO as oxidation product. A simple model was proposed for the amount of beryllium required to protect a AlMg melt solely on the Mg content. The amount of beryllium required was based on the log of the Mg content as shown in equation 1 by [9]:

$$Log(\%Be_{min}) = 85.7x10^{-3}(\%Mg) - 3.26 \quad (1)$$

The alloys AlMg5, AlMg10 and AlMg20 required 10, 20 and 150 ppm Be respectively to extend the time until the rapid increase in the oxidation rate occurred that is known as breakaway oxidation. The protection mechanism of Be was explained by the enthalpy of formation for BeO, the high diffusion rate of Be in Al melts and the molar volume expansion during the oxidation of Be to its oxide (Pilling-Bedworth ratio) [9]. The publication by [10] also concludes that BeO formation closes diffusion channels in the α-Al_2O_3 and MgO oxide layer. This can be summarised as oxide-stabilisation mechanism.

The work of [8] showed that an oxide layer containing BeO formed at the interface between the MgO layer and the liquid bulk metal. The exact composition of this layer was not verified, but it was shown that it contained a significant BeO fraction. It was shown that this oxide layer acted as a diffusion barrier between the melt and atmosphere/MgO layer slowing the oxidation and inhibiting breakaway oxidation. For solid alloys it was shown that a BeO containing phase formed preferentially at diffusion channels slowing the outward Mg diffusion. While the protective mechanism has been generally described, a number of questions exist such as the better understanding of minimum beryllium content required to protect a melt. [8]

Experiment procedure

Unalloyed Al99.85 and three different AlMg cast alloys and were produced with composition according to in Table 1

Table 1. Each melt was prepared in a six kg (13.2 lbs) crucible furnace with resistance heating at 750 °C (1382 °F). Beryllium was alloyed in increasing concentrations, also shown in Table 1

Table 1: Composition of alloys with main element composition analysed by Spark OES as well as classification to norm EN 573-3 and EN 1706. Elements not shown are according to norm.

DIN EN	Series name	Sample name	Element in wt%				
			Si	Fe	Mn	Mg	Be in ppm
EN AW-1085	Al99.85	Al	0.0293	0.03	0.00	0.00	< 1
		Al+3	0.0325	0.04	0.00	0.00	3
		Al+21	0.0338	0.04	0.00	0.00	21
EN AC-51100	AlMg3	AlMg3	0.27	0.20	0.18	3.02	< 1
		AlMg3+3	0.28	0.21	0.18	3.00	3
		AlMg3+6	0.28	0.20	0.18	2.97	6
		AlMg3+26	0.28	0.20	0.18	2.98	26
EN AC-51500	AlMg5Si2Mn	AlMg5	2.19	0.22	0.56	5.77	< 1
		AlMg5+3	2.20	0.22	0.56	5.80	3
		AlMg5+6	2.21	0.23	0.56	5.80	6
		AlMg5+23	2.19	0.22	0.55	5.69	23
EN AC-51200	AlMg10	AlMg10	0.05	0.43	0.02	9.19	< 1
		AlMg10+7	0.06	0.44	0.02	9.69	7
		AlMg10+22	0.07	0.44	0.02	9.73	22
		AlMg10+57	0.07	0.44	0.02	9.94	57

Sample casting and preparation

After achieving the required alloy composition and temperature, a tensile test cast bar was cast in a steel mold, pre-heated to ca. 300 °C (572 F), shown in Figure 1. The samples for subsequent thermogravimetric analysis (TGA) were cut out of the cast bar and the surface was milled completely to remove the naturally formed oxide skin during casting and normalise the surface area of the samples. Each sample had a height of 39 ± 1 mm and a diameter of 17 ± 0.1 mm. The weight of the samples was 22.4 – 23.6 g, depending on alloy density and resulting sample dimensions.

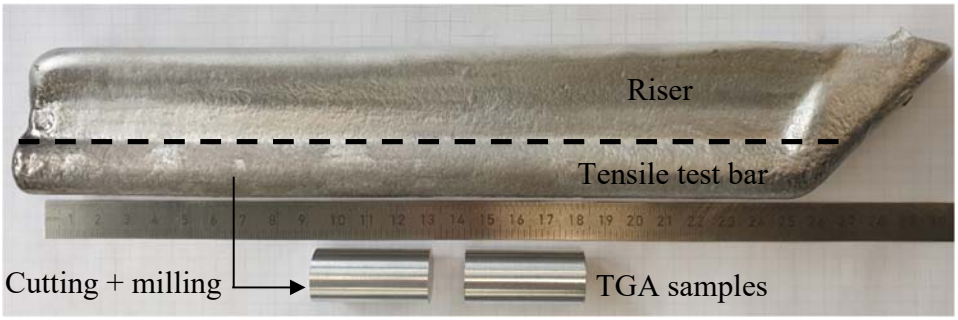

Figure 1: TGA samples prepared by cutting and milling out of a tensile test bar to remove the natural oxide skin and normalise the surface area.

Oxidation rate measurement by thermogravimetric analysis (TGA)

The TGA samples were cleaned with iso-Propanol as well as demineralised water and placed in high purity alumina crucibles. The crucibles with 15 mm diameter and 30 mm height were charged in an ELTRA TGA Thermostep thermogravimetric analyser with a weighing resolution of 0.0001 g and 0.02 % standard deviation. The device holds 19 samples and one empty reference crucible, allowing equal heating conditions and continuous weighing. During the oxidation rate measurement, the temperature was increased incrementally until reaching the holding temperature of 750 °C. The heating profile is given in Figure 2 to Figure 5 and was kept constant for all measurements. All experiments were performed in ambient air with a volume flow of 6 l/min through the heating chamber, providing a nearly constant O_2 partial pressure. In liquid state, all samples had an initial surface are of 6.16 cm² for oxidation. The weight gain over time of each sample was measured every 30 min. The measurement was repeated with three samples for each alloy (n = 3), if not stated otherwise in the results.

Oxide morphology characterization

Select samples were characterized to better understand the effects of beryllium. The AlMg10 alloy with 22 and 57 ppm were analysed by scanning electron microscope (SEM) with energy dispersive x-ray spectroscopy (EDS) X-ray photoelectron spectroscopy (XPS) and Auger electron spectroscopy (AES). The samples to be analysed were cut with an abrasive saw vertically in half to give a cross-section of the sample. One half of the sample was cast in epoxy and polished with standard metallography techniques. The second half was further cut to a 2 cm diameter disc to fit in the AES and XPS instruments. A Zeiss Supra SEM with an EDAX EDS was used to carry out a general investigation of the samples to understand the morphology of the oxide and metal. The presence of MgO or $MgAl_2O_4$ in the sample was determined by EDS using the Mg:O ratio where a 1:1 ration indicated MgO and a 1:4 ratio indicated $MgAl_2O_4$. AES and XPS was used for a detailed chemical composition analysis mainly in respect to identify any beryllium containing phases not detectable by EDS.

Element concentration analysis

Additionally, ICP-OES analysis was carried out with an Analytik Jena PQ 9000 Elite device to measure the Mg and Be concentrations before and after the experiments. Cut quarters of the samples AlMg10 with 22 and 57 ppm Be were used. For preparation, the samples were dissolved in nitric- and hydrochloric acid. All samples did completely go into solution, except the oxidised AlMg10+22 samples, due to the large oxide fraction. Therefore, the results describe an average element concentration through the sample and not only of the metal content.

Results and discussion

The thermogravimetric results are shown in Figure 2-5 as relative weight gain over time. Each data point represents the arithmetic average of three experiment repetitions (n = 3) if not stated otherwise in the figures. The heating chamber temperature is plotted as dashed line, according to the secondary y-axis. Additionally, the time of reaching liquid sample state is indicated by assuming it one hour after reaching the given liquidus temperature for each alloy.

Beryllium and pure aluminum

In Figure 2, the shown oxidation mass gain of Al99.85 aluminium is negligible at less than 0,04 %. The oxidation rate for the pure Al+2ppm Be and 21 ppm Be showed the same trend indicating that

Be has limited effect without the formation of an MgO and Al_2MgO_4 oxide layer for time periods up to 16 hours in the liquid state.

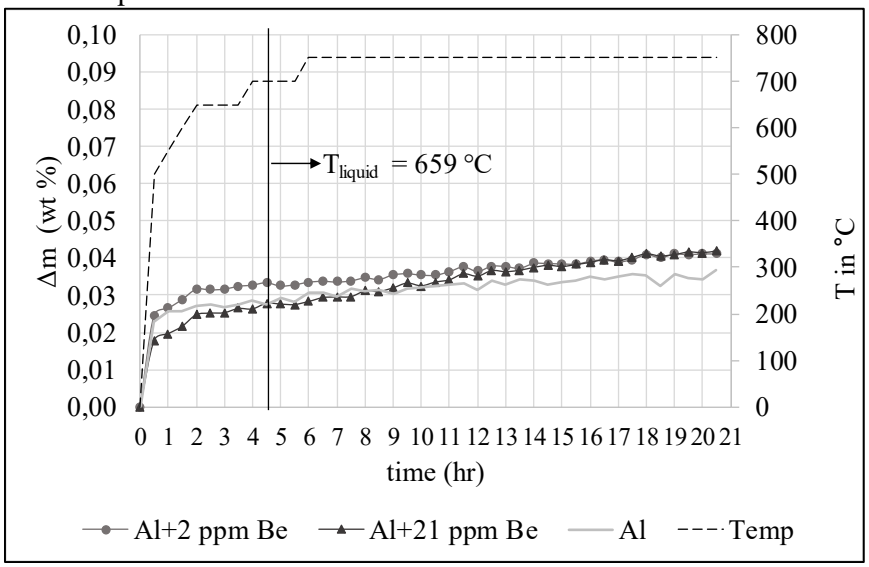

Figure 2: Relative oxidation rate (Δm/hr) of Al99.85 with different beryllium contents up to 750 °C holding temperature in air atmosphere.

Time dependence of Be on AlMg alloys

The effectiveness of beryllium is shown in Figure 3-5, additionally a time dependence is shown where Be's protective effect is lost after a longer holding time. The protective window is dependent on both the Mg and Be concentration. In this experiment setup, adding 3 ppm Be to an AlMg3 alloy significantly reduces the oxidation rate and 6 ppm or more will protect the alloy for more than 18 hours in liquid state.

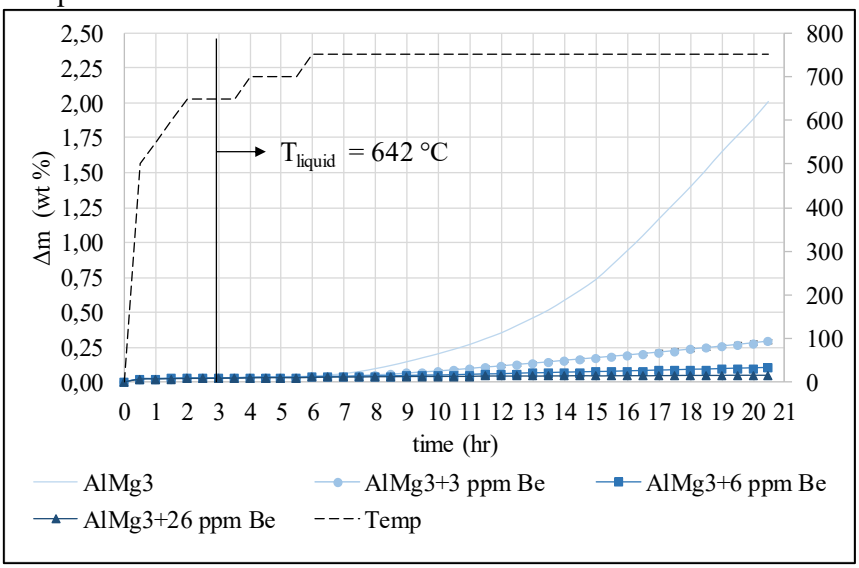

Figure 3: Relative oxidation rate (Δm/hr) of AlMg3 with different beryllium contents up to 750 °C holding temperature in air atmosphere.

The sensitivity of the oxidation rate to the Be concentration in AlMg5 melts is clearly shown in Figure 4. Where 2 ppm Be is sufficient to delay the onset of breakaway oxidation by two hours, and with 5 ppm the weight gain drops to 0,28 ± 0.09 % over 18 hours in the liquid state.

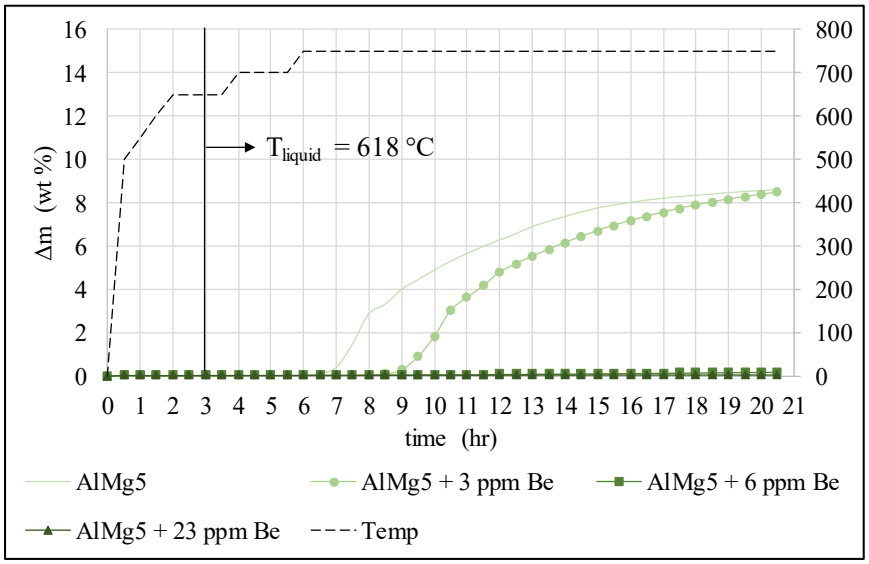

Figure 4: Relative oxidation rate (Δm/hr) of AlMg5Si2Mn with different beryllium contents up to 750 °C holding temperature in air atmosphere.

The time dependent protection mechanism of Be is again confirmed in Figure 5 with AlMg10. Due to the very high oxidation rate, even before reaching liquidus temperature, the average weight gain results showed a large standard deviation. The measurements were repeated with a second set of three samples, except for the AlMg10 alloy with 57 ppm Be.

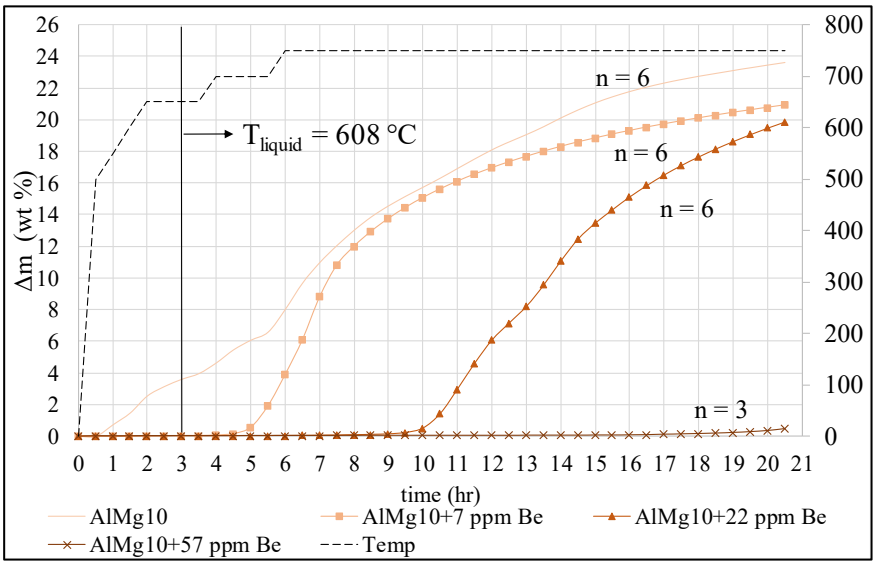

Figure 5: Relative oxidation rate (Δm/hr) of AlMg10 with different beryllium contents up to 750 °C holding temperature in air atmosphere

Oxide morphology characterization

The AlMg10 samples with 22 and 57 ppm Be showed significant variation in oxidation behaviour (20 % vs 1% respectively) as can be seen in Figure 5. Thus, these samples were investigated after oxidation to understand the differences between the sample morphology and how the protective abilities of Be are lost.

AlMg10 + 57 ppm Be

An overview of the cross-section is shown in Figure 6 where it can be seen that a large number of shrinkage pores are present and only a small region on the side of the sample shows oxide growth. It is seen clearly that 57 ppm Be is sufficient to protect this AlMg10 alloy. A uniformly thin oxide layer on the outer edge of the sample as shown in Figure 7. EDS analysis showed a Mg:O ratio of 1:1.13 clearly indicating an MgO layer. The MgO layer appears to be fractured and contains a number of pores which would indicate that it is a poor diffusion barrier. It is therefore assumed that the addition of 56 ppm of Be was sufficient to form a thin BeO diffusion barrier that lasted the entire oxidation time of the experiment.

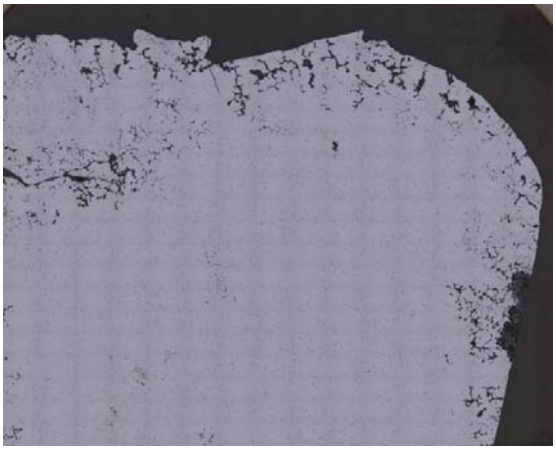

Figure 6: Polished cross-section of the AlMg10+57 ppm Be sample.

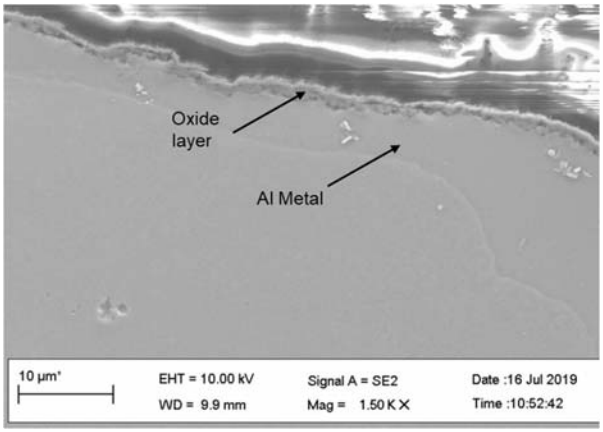

Figure 7: MgO layer formed on AlMg10+57 ppm Be sample after oxidation, in SEM SE mode.

AlMg10 + 22 ppm Be

The sample with 22 ppm of Be showed a marked difference from the 57 ppm Be sample as the sample lacked a uniform oxide layer on the surface and rather was a mix of oxide and metal as shown in Figure 8. EDS scans show that a majority of the oxide was $MgAl_2O_4$ which is to be expected given that the mass gain was 20 % which corresponds a nearly complete oxidation of the Mg to $MgAl_2O_4$ which would give a mass gain of 26 %. Select oxide phases had a notable amount of unoxidised metal trapped within the oxide as droplets. A large void was found to form under the sample. The remaining metal phase accounts for only 25-30 % of the cross-sectional sample area. With much of the unoxidised aluminium metal being found trapped in a mixed phase of $MgAl_2O_4$ and Al metal.

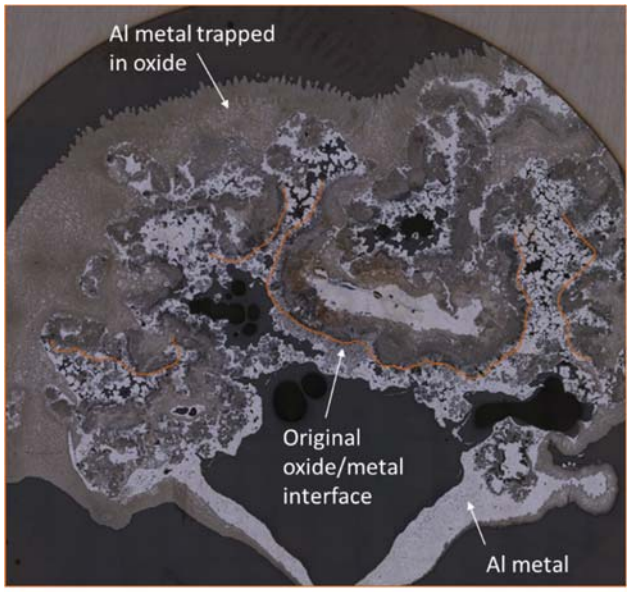

Figure 8: Cross-section of the AlMg10+22 ppm Be sample, with the lightest phase being Al metal and darker phases being $MgAl_2O_4$ with various amounts of Al metal mixed in.

Analysis of the sample containing 22 ppm Be via AES and XPS showed no signs of a Be or BeO containing phase in any of the points checked. Multiple points on the sample were check by both methods. Special focus was paid to the region where the initial oxide-metal interface existed as based on previous research [8] as the most likely location of any Be/BeO phase.

Mg and Be element concentration

As no phase containing Be could be identified on the sample the composition was checked by ICP-OES. A Be content in the same range as the original concentration indicates little or no depletion as shown in Table 2.

Table 2: ICP-OES results of samples before and after oxidation (analysis repeated twice for post oxidation sample).

Element	AlMg 10+22 ppm Be			AlMg 10+57 ppm Be		
	initial	final	final	initial	final	final
Be (ppm)	23	27	25	62	65	57
Mg (wt %)	10.5	4.8	6	10.2	9.7	10.1

Beryllium protection model

The results show that adding just 2 ppm Be to an AlMg5 alloy delays the time until breakaway oxidation by two hours and 5 ppm delays the onset till longer than 21 hours. Thus, the required Be content is not only dependent on the Mg content, but also the holding time. Figure 9 shows the required Be concentration to protect a melt as a function of time for AlMg3, AlMg5 and AlMg10. For the purpose of this work protection is assumed to be a mass gain below 0.1%. While mass gains below 0.1 % are not obtainable for Mg alloys in industrial furnaces, at the laboratory scale an increase above 0.1 % was a clear indication of the start of breakaway oxidation. In this work, the pure Al samples show less than 0.1 % mass gain for all time and are therefore not included.

Figure 9 shows a linear protection time vs Be content, though the number of data points is limited. The slope of the line is connected to both Mg and Be concentration where the constant where the line crosses the y-axis is dependent only on the Mg content and indicates the breakaway time for a Be-free alloy.

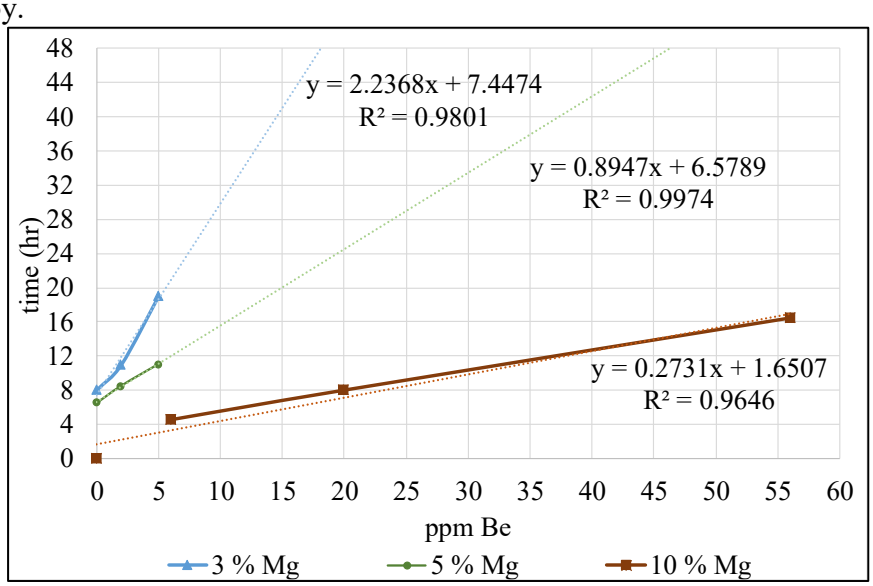

Figure 9: Linear model for required beryllium content to protect a melt for a desired period of time dependent on the magnesium content.

A direct comparison of the model proposed by [9] is not possible, as it proposed a logarithmic relationship based on the Mg content with no time variable. If the required Be concentrations from

equation (1) are used in the current model a varying protection time is found as shown in Table 3. As metal is rarely held for periods of 12.5 hours or longer it can be said that equation (1) overestimates the required Be amounts compared to the current results.

Table 3: Necessary Be content based on logarithmic model by [9] compared to protection period by linear model in this work.

Mg in wt%	Be used by [9] in ppm	Protection in hours according to linear model in Figure 9
3	10	30
5	15	20
10	40	12.5

Discussion

A clear mechanism explaining how the Be protective effect is lost is not apparent from the results above, however, further insights can be made in to the Be protective mechanism. Firstly, a lack of Be depletion shows that the loss of protection is not dependent solely on the Be concentration. Rather another time dependent variable must be at play. This second variable will result in the rupturing of the protective BeO layer resulting in breakaway oxidation. This means that while Be concentration is important in determining the protectiveness of the BeO layer, the ultimate failure of the layer is depended on another yet undetermined variable.

The lack of Be depletion shows that the BeO layer will reach a limiting thickness in which the the layer will act as a barrier preventing diffusion of Be out and oxygen in, limiting the layers growth. Once the protective layer is ruptured, the high concentration of Mg results in a rapid oxidation such that a new protective layer is not able to form. It should be noted that any flow or turbulence in the liquid metal will cause a variation in the concentration gradient and potentially affect the time it takes for the BeO layer to rupture. To date, no knowledge exists on the thickness of a BeO layer, even if [8] reported a thickness of 40 nm for a 100 ppm Be, but the thickness at lower concentrations is unknown.

The results above give insight on how to tailor beryllium usage to have the highest possible effect with the lowest Be usage. For industrial applications, the time until breakaway oxidation and the required beryllium concentration to extend the onset of breakaway oxidation to beyond the end of a cast is of high interest. For example, the holding cycle of a casting furnace in a foundry could be up to eight hours in a shift without production, however, it may be as short as a few hours. The melt cleanliness has to be maintained and extensive oxidation avoided during the entire holding cycle. Thus, to determine the minimum required Be content, both the cycle time and Mg content should be considered.

Conclusions

The effects of varying beryllium concentrations on the onset time for breakaway oxidation on AlMg melts was clearly shown through TGA experiments. It was shown that:

1. Be has no clear effect on the oxidation mass gain of Mg free alloys.
2. The protective effect of Be is time dependent based on both the Mg and Be concentration

3. No significant Be decrease in the melt was seen after oxidation for 21 hours.
4. The location of any Be containing phases in the samples that experienced breakaway oxidation is not known.

Based on the results above, a simple linear model was proposed to allow determination of the required beryllium content based on the Mg concentration and required protection time. This work allows for the beryllium usage to be minimized until a suitable replacement alloying element can be identified.

Acknowledgement

This work has been partly funded by the SFI Metal Production, (Centre for Research-based Innovation, 237738). The authors gratefully acknowledge the financial support from the Research Council of Norway and the partners of the SFI Metal Production. We also thank TRIMET Aluminium SE (Essen, Germany) for support.

References

[1] Bundesverband der Deutschen Gießerei-Industrie, "Aluminium-Guss" (Gießerei-Verlag, Düsseldorf, 2013), 133-143.
[2] F. Ostermann, Anwendungstechnologie Aluminium, (Springer-Verlag Berlin Heidelberg, 2014), 185
[3] D. Altenpohl, "Aluminium und Aluminiumlegierungen" (Springer Verlag, Berlin, 1956), 658-659.
[4] L. F. Mondolfo, Escherle, "Aluminium Alloys: Structure and Properties" (Butter Worth & Co Ltd., London, 1976), 231-233.
[5] WorkSafe New Zealand, "Workplace Exposure Standard (WES) review Beryllium" (Wellington, New Zealand, 2018) 8-15.
[6] EN 1706, "Aluminium and aluminium alloys – Castings" (DIN Deutsches Institut für Normung e. V., Beuth Verlag GmbH, Berlin, 2019), 14-17.
[7] The Aluminium Association, Designations and Chemical Composition Limits for Aluminum Alloys in the Form of Castings and Ingot, Arlington, USA, October 2018
[8] N. Smith, PhD Thesis, NTNU, 2019
[9] W. Thiele, "Die Oxydation von Aluminium-und Aluminiumlegierungsschmelzen" (Aluminium, Vol. 38, 1962), 780-786.
[10] K. Wefers, "Properties and Characterization of surface oxides on aluminum alloys" (7th International Light Metals Congress, Leoben and Vienna, 1981).